WORLD JOURNAL OF PHARMACEUTICAL RESEARCH
Coden USA: WJPRAP Impact Factor 8.63
Volume 15, Issue 18, 659-676. Research Article ISSN 2277–7105

DESIGN, SYNTHESIS, CHARACTERIZATION AND DOCKING STUDY OF NOVEL PYRIDINE DERIVATIVES AS ANTITUBERCULAR ACTIVITY

[1]Teli Rahul V., [1]Suprita N. Vibhutihalli, [1]Samiksha A. Aitawade, [1]Suprita M. Awati, [1]Pavitra Nidagundi, [1*]Somashekhar M. Metri

[1*]Department of Pharmaceutical Chemistry, BLDEA's Shri Sanganabasava Mahaswamiji College of Pharmacy and Research Centre, Vijayapura, Karnataka- 586103.

Article Received on 12 August 2026,
Article Revised on 02 Sept. 2026,
Article Published on 16 Sept. 2026,

https://doi.org/10.5281/zenodo.22767730

***Corresponding Author**
Somashekhar M. Metri

Department of Pharmaceutical Chemistry, BLDEA's Shri Sanganabasava Mahaswamiji College of Pharmacy and Research Centre, Vijayapura, Karnataka- 586103.

How to cite this Article: [1]Teli Rahul V., [1]Suprita N. Vibhutihalli, [1]Samiksha A. Aitawade, [1]Suprita M. Awati, [1]Pavitra Nidagundi, [1*]Somashekhar M. Metri (2026). Design, Synthesis, Characterization And Docking Study Of Novel Pyridine Derivatives As Antitubercular Activity. World Journal of Pharmaceutical Research, 15(18), 659–676.

ABSTRACT

The present study was undertaken to design, synthesize, characterize, and evaluate novel pyridine derivatives for their potential antitubercular activity. Pyridine-4-carbohydrazide was prepared from pyridine-4-carboxylic acid and subsequently used for the synthesis of novel derivatives, including PR4SII-A, PR4SII-B, and PR4SII-C. The synthesized compounds were characterized using spectroscopic techniques including IR, ^{1}H-NMR, ^{13}C-NMR, and mass spectroscopy. In-silico drug-likeness, ADMET, toxicity prediction, and molecular docking studies were performed to assess their pharmacokinetic properties, preliminary safety profile, and interaction with the antitubercular target dihydrofolate reductase (PDB ID: 1DF7). Among the synthesized compounds, PR4SII-B exhibited the most favorable docking score of −8.3 kcal/mol, showing interactions with ASP A:27, TRP A:6, SER A:49, PHE A:31, and ILE A:14. The antitubercular activity of PR4SII-A and PR4SII-B was evaluated against *Mycobacterium tuberculosis* H37Rv using the Microplate Alamar Blue Assay (MABA). Both compounds demonstrated concentration-dependent inhibition of mycobacterial growth. At 100 µg/mL, PR4SII-A showed 61.79% inhibition with an IC_{50} of 73.74 µg/mL, whereas PR4SII-B showed 65.09% inhibition with an IC_{50} of 67.24 µg/mL. Overall, PR4SII-B demonstrated comparatively better docking performance and in-

vitro antitubercular activity than PR4SII-A, indicating that it may serve as a promising lead for further investigation as an antitubercular agent.

KEYWORDS: Pyrimidine, Isoniazid, Insilco study, ADME Analysis, Anti-TB activity.

GRAPHICAL ABSTRACT

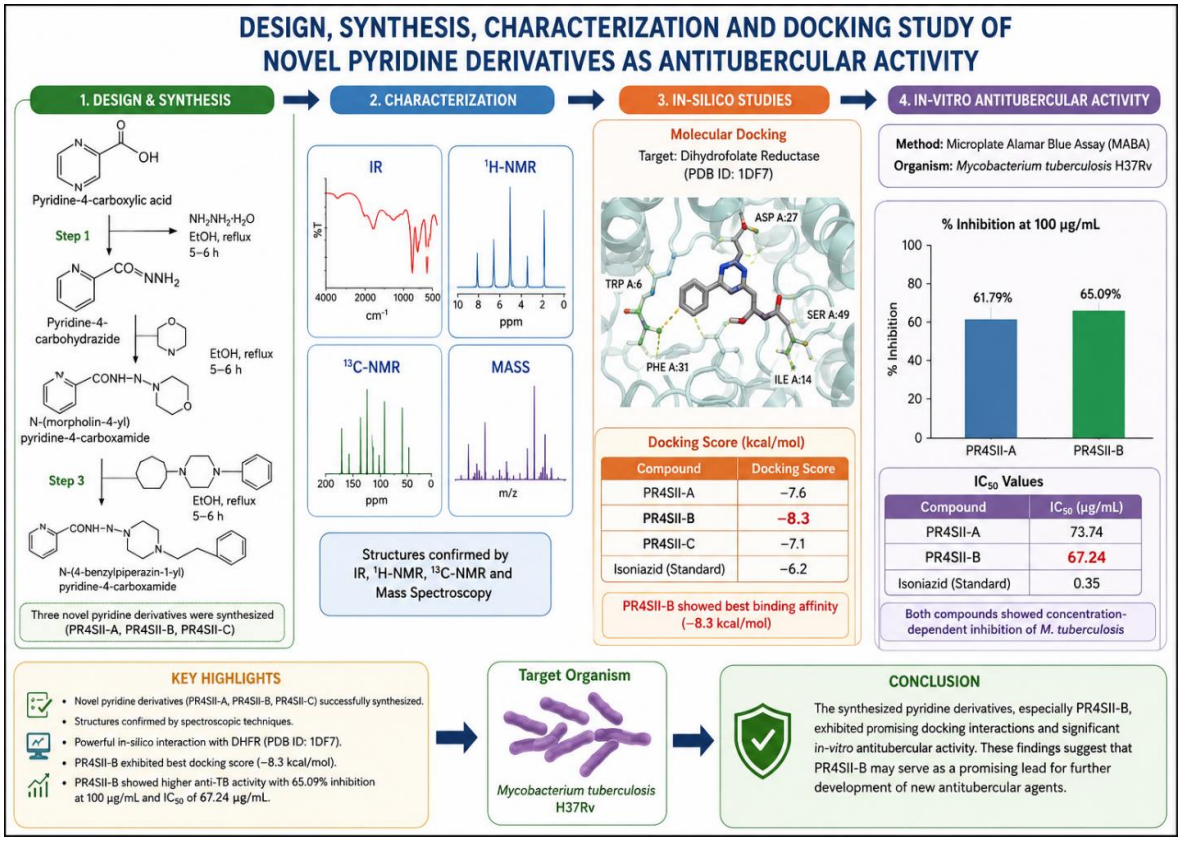

INTRODUCTION

Pyridine-based compounds exhibit promising anti-tubercular activity through several mechanisms that interfere with the survival and multiplication of Mycobacterium tuberculosis. The biological activity of these compounds is strongly influenced by the nitrogen atom present in the pyridine ring, which contributes to hydrogen-bonding interactions, protonation, and binding with essential bacterial enzymes and cellular targets.[1] Depending on their molecular structure and substituents, pyridine derivatives may inhibit enzymes involved in mycobacterial cell-wall synthesis, nucleic-acid metabolism, energy production, or other essential biochemical pathways. Some pyridine-containing anti-tubercular agents can interfere with the synthesis of mycolic acids, which are important components of the highly hydrophobic cell wall of M. tuberculosis. Inhibition of these pathways weakens the bacterial cell envelope and ultimately affects bacterial viability. Other

derivatives may undergo metabolic activation within the mycobacterial cell to form reactive intermediates that interfere with vital cellular processes.[2] The lipophilic and polar characteristics of pyridine derivatives can also influence their penetration into the mycobacterial cell and their interaction with intracellular targets. Therefore, structural modification of the pyridine nucleus provides an important strategy for developing potent anti-tubercular compounds with improved selectivity, pharmacokinetic properties, and activity against drug-resistant strains of M. tuberculosis.[3]

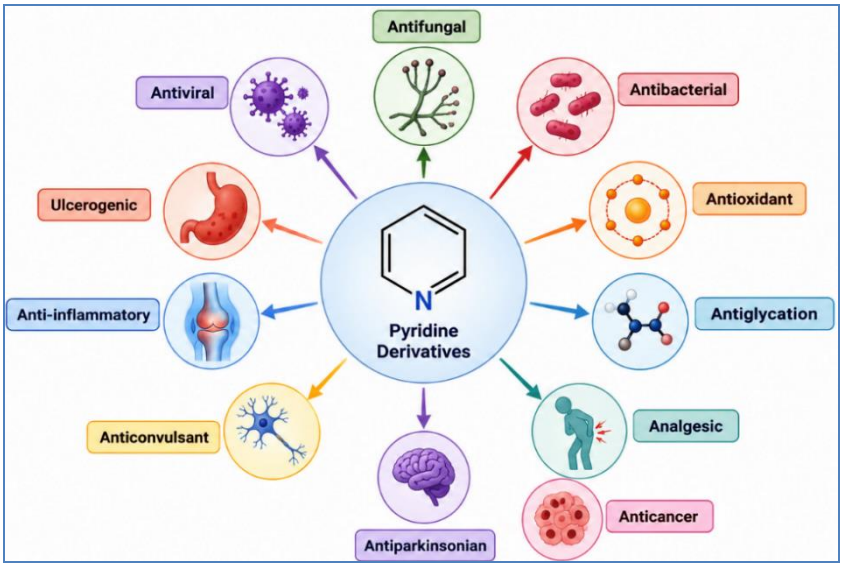

Figure No 1: Applications of Pyridine.

MATERIALS AND METHODOLOGY

SCHEME

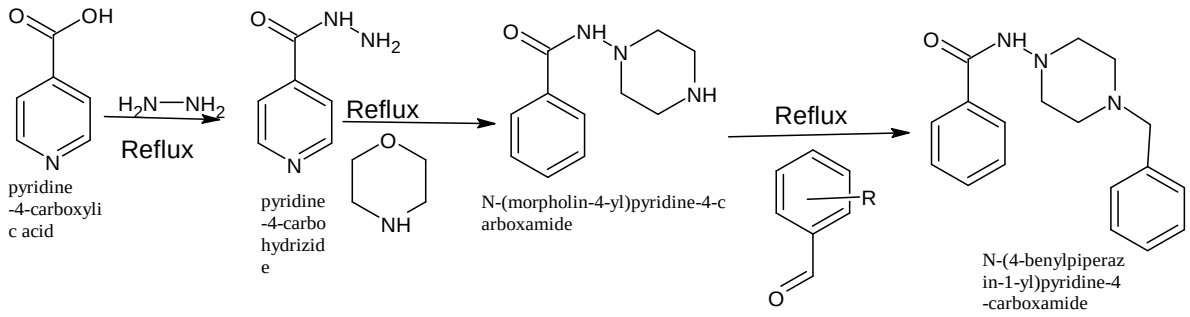

Step 1: Preparation of pyridine-4-carbohydrazide from pyridine-4-carboxylic acid.

Take a pyridine-4 carboxylic acid in a round bottom flask and add a solution of 100 ml ethanol and add small amount of conc.H_2SO_4 as a catalyst and attached reflux condenser and reflux the mixture for about 5-6 hours. After then allow the reaction mixture to cool and neutralized carefully with suitable base. Then The product was filtered. The purity of the

product was confirmed by a single spot on TLC plate percentage yield (%) is 81.39%, Melting Point is 306.1℃ and Rf Value is 0.65.[4-5]

Step 2: Preparation of N-(morpholin-4-yl) pyridine-4-carboxamide from pyridine-4 carbohydrazide

To the above intermediate, add morpholine appropriate molar proportion and add a suitable solvent such as ethanol attached reflux for 5-6 hours and after the cooling reaction mixture add poured on crushed ice and filtered off. The product was obtained. The purity of compound was confirmed by a single spot on TLC plate. percentage yield (%) is 83.33%, Melting Point is 134.28℃ and Rf Value is 0.80.[6]

Step 3: Preparation of N-(4-benzylpiperazin-1-yl) pyridine-4-carboxamide from N-(morpholin-4-yl) pyridine-4-carboxamide

To the above intermediate aromatic halide was added drop wise with constant stirring the reaction mixture was reflexed for 5 to 6 hours and cool the reaction and evaporate the reaction mixture with rotary evaporator the product was obtained the purity of compound was confirmed by a single spot on TLC plate. percentage yield (%) is 80.85%, Melting Point is 134.35℃ and Rf Value is 0.50.[7]

Figure No 2: Synthesis of Pyridine derivatives.

Docking

Docking studies were carried out to analyse the different types of biomolecular interactions and ligand receptor binding affinities. The docking studies were carried out by means of Autodock 1.5.7 Tools, Biovia Discovery Studio 2020, and PyMOL. The docking study was performed on proteins mely crystal structure of antitubercular protein Di hydro folate Reductase (PDB id:1DF7).[8-9]

Protein preparation

The crystal structure of antitubercular protein Di hydro folate Reductase (PDB id:1DF7) was retrieved from the RCSB Protein Data Bank, the protein was prepared by removing the water molecules, adding polar hydrogens and Kollmann charges using Autodock 1.5.7 Tools, the prepared proteins were saved in PDBQT format.[10]

Ligand Preparation

The ligand's 2D structures were initially created using ACD ChemSketch and stored in the MDL MOL file format. These structures were then transformed into 3D conformations and saved in PDB format with the help of Open Babel software. The resulting PDB files were later imported into AutoDockVina, where each molecule underwent preparation for molecular docking. In this preparation phase, the structures were converted into the PDBQT format, which is necessary for docking simulations in AutoDockVina. Ligands were converted to PDBQT format with defined rotatable bonds and Gasteiger charges. A grid box was set around the active site, and docking was run with default parameters. Binding affinities and key ligand–residue interactions were analyzed.[11-12]

Evaluating Docking Results

Docking results from AutoDockVina were assessed based on binding affinity scores (kcal/mol), with more negative values indicating stronger predicted binding. Top poses were selected by comparing binding energies and analyzing key interactions such as hydrogen bonds, hydrophobic contacts, and π-π stacking with active site residues. Ligand–protein interactions were visualized using Discovery Studio Visualizer and PyMOL, enabling detailed inspection of binding conformations and interaction profiles, thus providing insights into binding efficiency and potential biological relevance.[13]

RESULT AND DISCCUTION

INSILICO STUDIES

Table No. 2: Structures of Derivatives.

Compound Code	Structures	Molecular Weight
Isoniazide	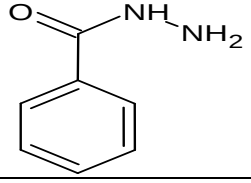	136.15 gm/mol

PR4SII-A	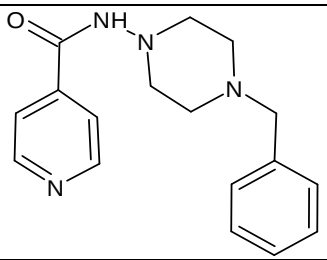	296.37 gm/mol
PR4SII-B	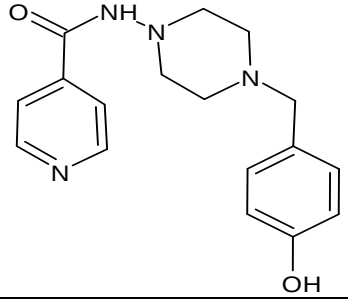	321.37 gm/mol
PR4SII-C	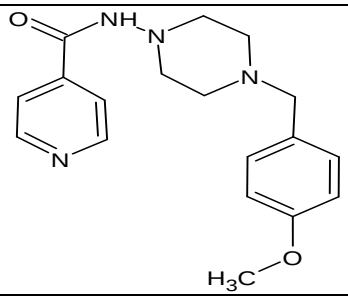	326.39 gm/mol

Table No. 3: Drug Likeness and ADMET Studies.

Compound Code	MW	HD	HA	WLOG P	ESOL	BBB	GI	Bio-availability	TPSA	Hepatotoxicity
Isoniazide	136.15	2	2	0.29	-1,12	No	high	0.55	55.12	0.83
PR4SII-A	296.37	1	4	0.63	-2.80	No	high	0.55	48.47	0.61
PR4SII-B	321.37	2	5	0.34	-2.66	No	high	0.55	68.70	0.56
PR4SII-C	326.39	1	5	0.64	-2,87	No	high	0.55	57.70	0.60

Table No. 4: Toxicity level Prediction.

Compound	Acute inhalation toxicity	Acute oral toxicity	Acute Dermal toxicity	Eye irritation & corrosion	Skin sensitization	Skin irritation &corrosion
Isoniazide	Non-toxic 74.0%	Toxic 79.0%	Non-toxic 60.0%	Non-toxic 80.0%	Non sensitizer 60.0%	Negative 90.0%
PR4SII-A	Non-toxic 66.0%	Toxic 72.0%	Non-toxic 75.0%	Toxic 52.0%	Non sensitizer 70.0%	Negative 80.0%
PR4SII-B	Non-toxic 79.0%	Toxic 56.0%	Non-toxic 85.0%	Toxic 55.0%	Non sensitizer 70.0%	Negative 70.0%
PR4SII-C	Non-toxic 75.0%	Toxic 73.0%	Non-toxic 79.0%	Toxic 61.0%	Non sensitizer 70.0%	Negative 80.0%

PR4SIIB demonstrates a comparatively favorable toxicity profile for inhalation and dermal exposure. The compound is predicted to be non-toxic by the acute inhalation route, with a

confidence of 79%. Its acute dermal toxicity is also predicted to be non-toxic, with the highest confidence of 85% among the reported endpoints. These predictions suggest that PR4SIIB may have a lower acute toxicity potential through inhalation and dermal exposure. However, PR4SIIB is predicted to be toxic following acute oral exposure, with a confidence of 56%, indicating as certain but potentially important oral toxicity concern. The compound is also predicted to show eye irritation/corrosion potential, with a toxicity prediction of 55%.In contrast, PR4SIIB is predicted to be a non-sensitizer for skin sensitization (70%) and negative for skin irritation/corrosion (70%). Overall, the strongest favourable predictions for PR4SIIB are its non-toxic dermal (85%) and inhalation (79%) profiles. Therefore, among the endpoints assessed, PR4SIIB appears particularly favorable with respect to acute dermal and inhalation toxicity, although oral and ocular effects require further attention. Because these are in-silico predictions, they should be interpreted as evidence of potential hazard rather than definitive experimental toxicity; model validity, applicability domain, and uncertainty should be considered before drawing final safety conclusions.

Table No. 5: Similarity Of Distribution of Derivative PR4SIIB(Acute Oral Toxicity)

Compound	End point	Prediction	Confidence	Applicability Domain	Predicted fragment contribution
PR4SIIB	Acute oral toxicity	Toxic (+)	56.0%	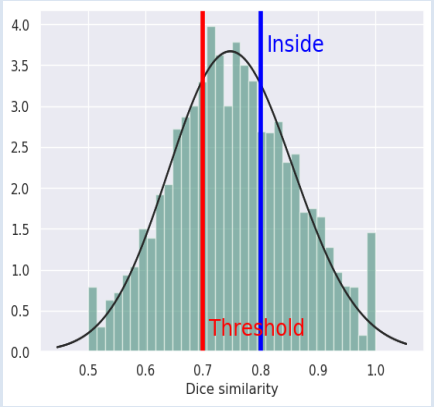	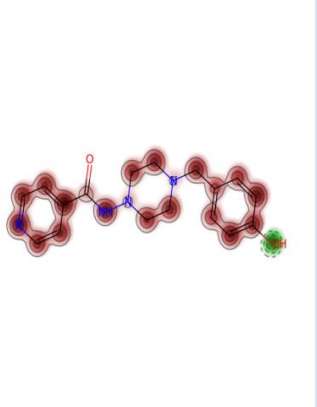

The in-silico toxicity profile of the synthesized compound was evaluated using a computational toxicity prediction approach. The compound was predicted to exhibit acute oral toxicity under the applied prediction model. The obtained prediction was classified as PR4S II-B, indicating a predicted toxicity category based on the model criteria. The probability associated with this prediction was 56.0%, suggesting a moderate level of confidence in the predicted classification. The similarity distribution plot demonstrates the structural relationship of the investigated compound with compounds present in the reference dataset. The compound was located within the defined threshold region ("Inside") of the

similarity distribution. This observation indicates that the prediction is supported by compounds having comparable structural features. The result provides an early indication of the potential oral toxicity of the compound before experimental toxicological evaluation. However, computational predictions should be considered preliminary and should not replace appropriate experimental toxicity studies. Overall, the predicted acute oral toxicity profile provides useful information for assessing the preliminary safety characteristics of the synthesized compound.

Table No. 6: Similarity Of Distribution of Derivative PR4SIIB (Eye Irritation & Corrosion)

Compound	End point	Prediction	Confidence	Applicability Domain	Predicted fragment contribution
PR4SIIB	Eye irritation & corrosion	Toxic (+)	55.0%	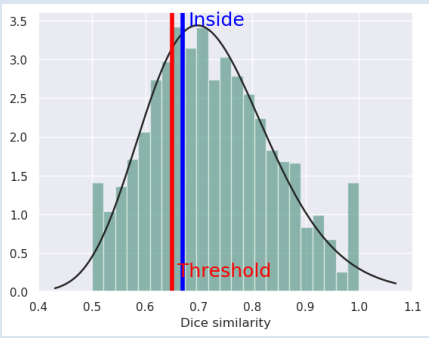	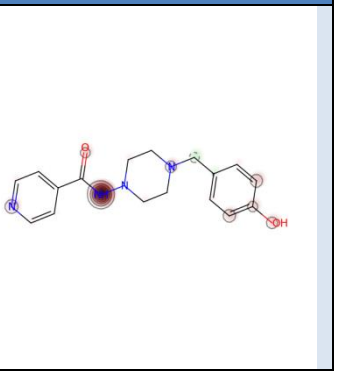

The synthesized compound was subjected to an in-silico toxicity assessment to predict its potential for eye irritation and corrosion. The predicted endpoint was eye irritation and corrosion, indicating a potential adverse effect on ocular tissues. The computational model classified the compound as Toxic (+) for the investigated endpoint. The prediction was obtained with a 55.0% confidence level, indicating moderate confidence in the computational result. The applicability-domain analysis showed that the compound was positioned inside the applicability domain of the prediction model. This finding suggests that the compound possesses structural characteristics comparable to compounds represented in the model's reference dataset. The predicted fragment contribution further indicates that specific structural fragments of the molecule contribute to the estimated toxicity outcome. The result provides preliminary information regarding the possible ocular safety concerns associated with the synthesized compound. Since the prediction is computational and has moderate confidence, the result should be interpreted cautiously and validated using appropriate experimental studies. Overall, the in-silico analysis suggests a potential eye

irritation/corrosion risk, which should be considered during further safety and biological evaluation of the compound.

Molecular Docking Study and Visualization of Interaction

Binding energy suggests the ligand affinity and strength of interaction with the target protein, a compound with a lower binding energy is preferred as a possible drug candidate because that will generate a competitive and reversible inhibitor the compound with the highest binding score PBNS-IA with -6.5 and PBNS-IB with -7.9 showed similar binding to amino acid residues in the active pocket as compare with standard streptomycin.

Table No. 7: Ligand-Protein1DF7 interaction.

Compound	Binding score	Interacted residues
ISONIAZIDE	-4.5	ILE A: 14 TYR.A: 100 GLY A: 96 ALA A: 7
PR4SII-A	-5.9	ALA A: 126 GLY A: 18 LEU A: 127 ARG A: 45
PR4SII-B	-8.3	ASP A: 27 TRP A: 6 SER A: 49 PHE A: 31 ILE A: 14
PR4SII-C	-5.7	GLY A: 12 LEU A: 127 PRO A: 129 TYR A: 156

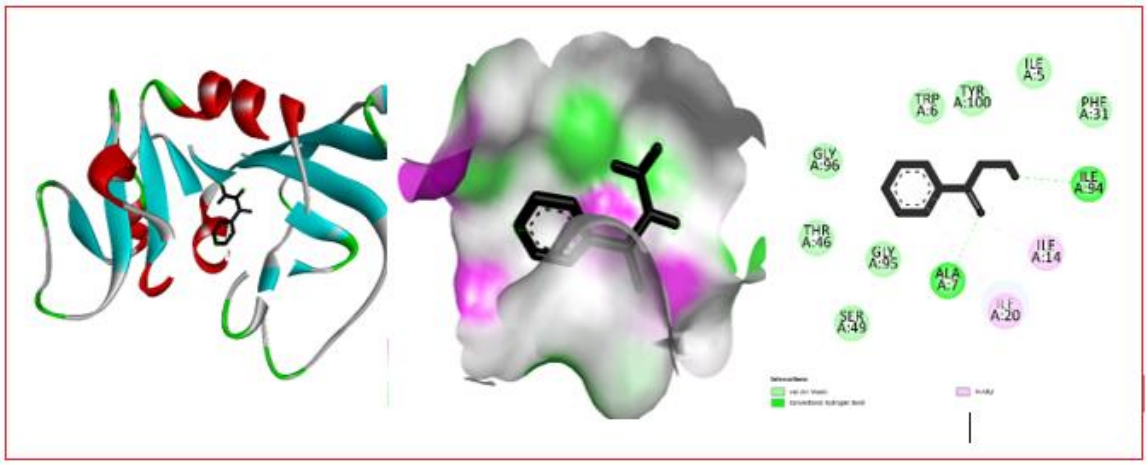

Figure No. 3: Interaction between ligand Isoniazid & Protein 1DF7.

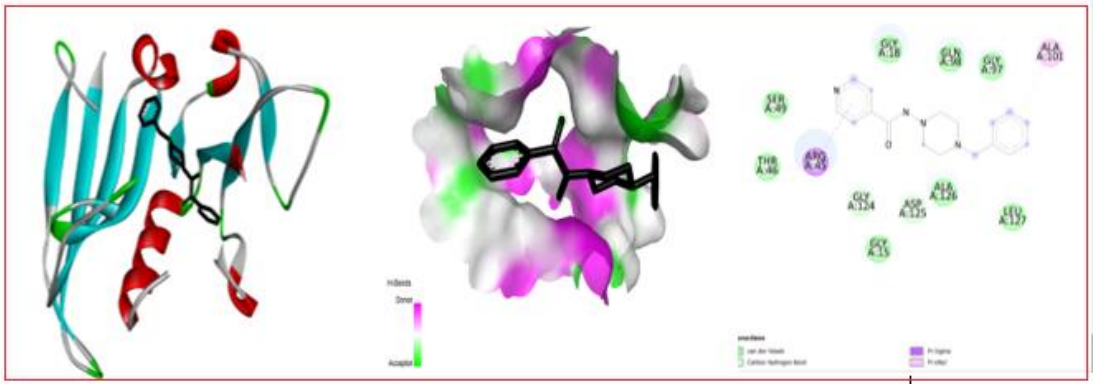

Figure No. 4: Interaction between ligand & Protein 1DF7 PR4SII-A.

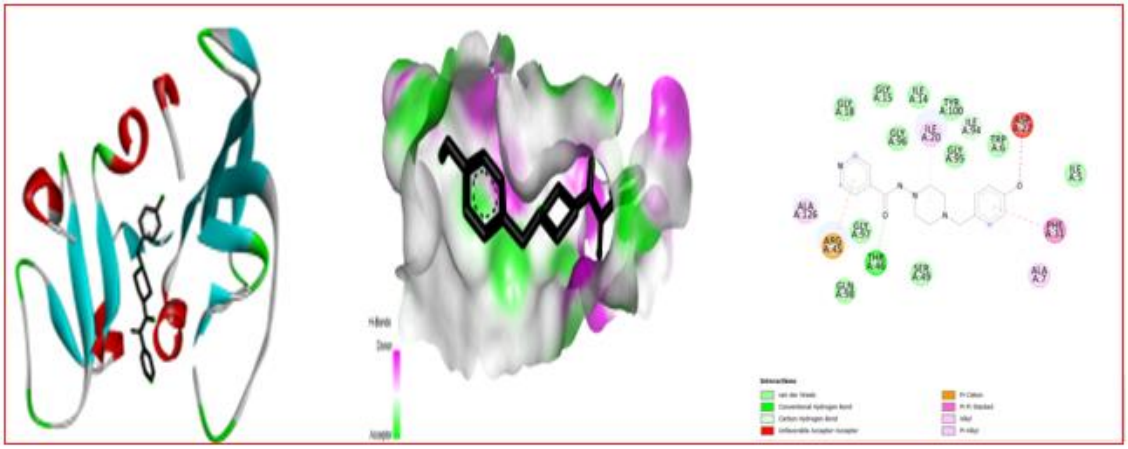

Figure No. 5: Interaction between ligand & Protein 1DF7 PR4SI1-B.

Characterization

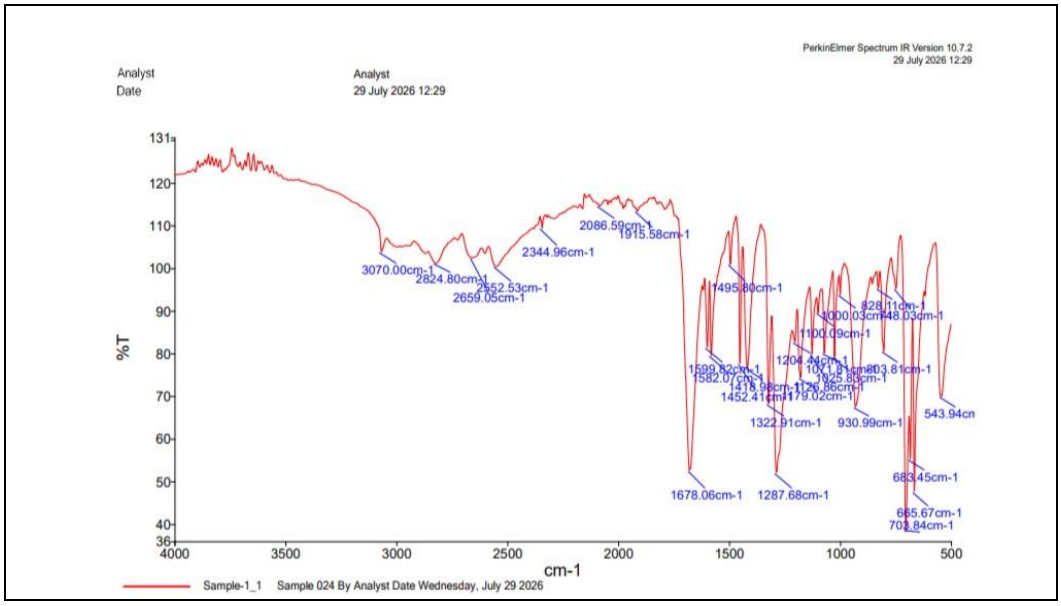

Figure No. 6: IR Spectroscopy of PR4SI1-B.

Table No. 8: IR Spectroscopy of PR4SI1-B.

Type of vibrations	Group Frequency in wave number (cm^{-1})
O-H Stretching	3070cm-1
Aliphatic C-H stretching	2924cm-1
Aromatic C=C Stretching	1628cm-1
C=C Stretching	2091cm-1
C-H Bending	1452cm-1
C-O Stretching	1277cm-1
C=C Bending	945cm-1

1H-NMR Spectroscopy

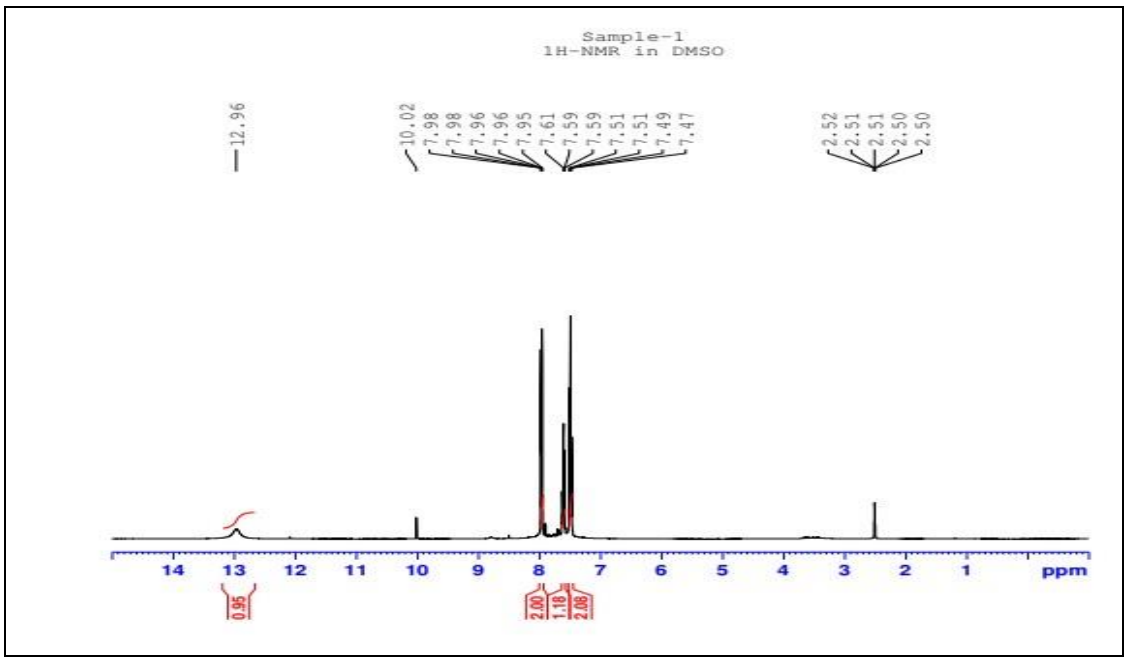

Figure No.7: ^{1}H NMR Spectrum of compound PR4SI1-B.

Table No. 9: 1H NMR Spectrum of compound PR4SI1-B.

Peak Assigned (Multiplicity)	δ Value (ppm)
OH (singlet)	10.02-12.96
CH_2(doublet)	2.5-3.5
-CH_2(doublet)	3,5-4.0
Ar-H (multiplet)	7.47-7.61
Ar-H(multiplet)	7.95-7.98

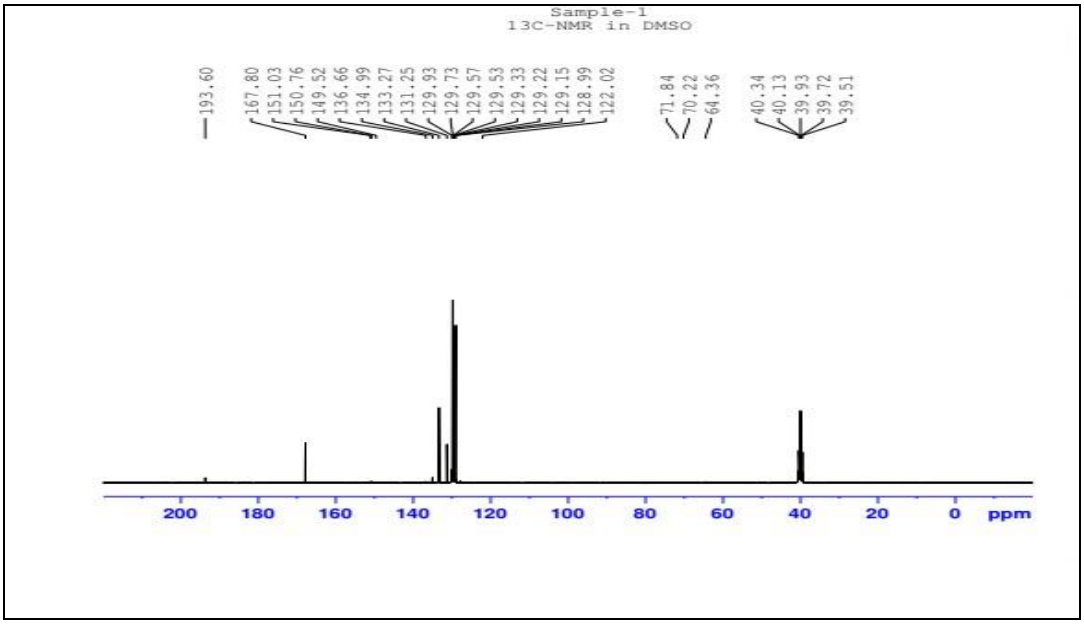

Figure No. 8: ^{13}C-NMR Spectroscopy of compound PR4SI1-B.

Table No. 10: 13C NMR Spectrum of compound PR4SI1-B.

Peak Assigned (Multiplicity)	δValue (ppm)
-C-OH (singlet)	193.60
-CH_2(triplet)	64.36-71.84
-CH_2(doublet)	39.51-40.34
Ar-H(multiplet)	121.25-167.80

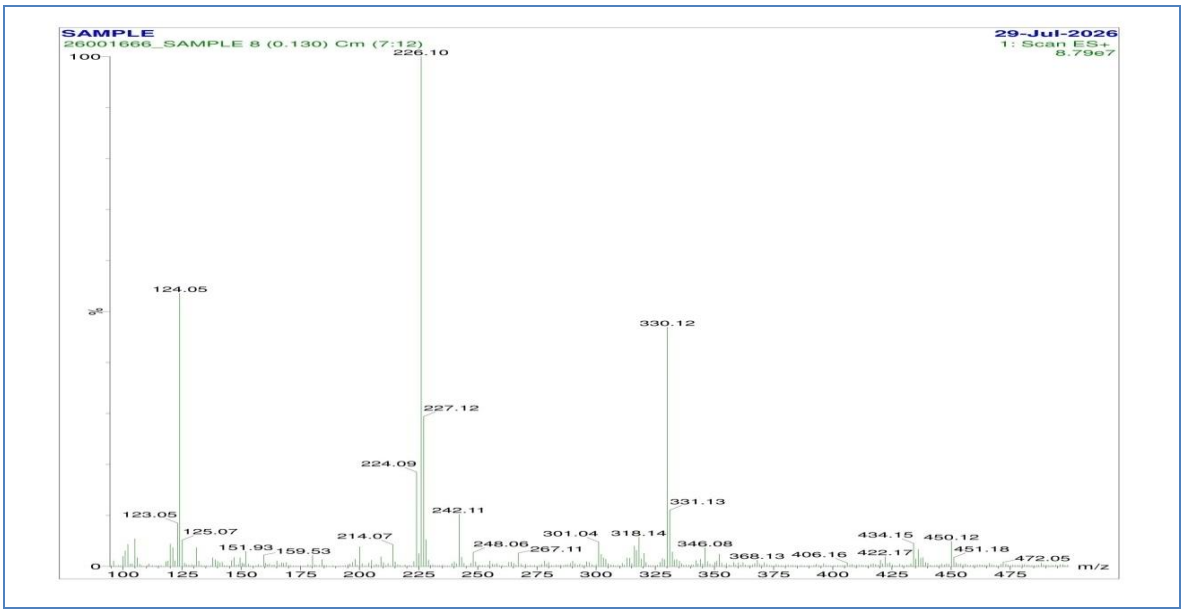

Figure No. 9: Mass Spectroscopy of compound PR4SI1-B.

- M^+ Peaks (Mass Peak) at m/z 330.12and base Peak is 226.10Molecular weight of the compound (PR4SII-A) is 330.12m\z

ANTITUBERCULAR ACTIVITY BY MICRO PLATE ALAMAR BLUE ASSAY (MABA)

PROCEDURE

The antitubercular activity of the test sample was evaluated against Mycobacterium tuberculosis H37Rv using the Microplate Alamar Blue Assay (MABA) under aseptic conditions. The assay was performed in sterile, flat-bottom 96-well microplates using Middlebrook 7H9 broth supplemented with 10% OADC (Oleic acid–Albumin–Dextrose–Catalase) enrichment and 0.05% Tween-80. Briefly, 100 µL of supplemented Middlebrook 7H9 broth was dispensed into each well. The test sample was dissolved in dimethyl sulfoxide (DMSO)/respective solvent and obtained final concentrations ranging from 20-100 µg/mL. The final concentration of DMSO in the assay did not exceed 1% (v/v) to avoid inhibition of bacterial growth.[14-15]

A standardized inoculum of M. tuberculosis H37Rv equivalent to approximately 1×10^5 CFU/mL was prepared from a freshly grown culture and 100 µL was added to each test well, giving a final assay volume of 200 µL per well. Rifampicin at appropriate concentrations were included as positive controls, while growth control wells (medium with bacterial inoculum) and sterile control wells (medium only) served as negative and blank controls, respectively. The microplates were sealed and incubated at 37°C for 7 days under appropriate biosafety conditions.[16-17]

Following incubation, 20 µL of Alamar Blue reagent and 12.5 µL of 20% Tween-80 were added aseptically to each well. The plates were further incubated for 24 h at 37°C. The color change measured spectrophotometrically at 600 nm. A change in color from blue to pink indicated bacterial growth, whereas wells remaining blue indicated inhibition of mycobacterial growth. The Minimum Inhibitory Concentration (MIC) was defined as the lowest concentration of the test sample that prevented the color change from blue to pink, indicating complete inhibition of visible bacterial growth. All experiments were performed in triplicate, and the results were expressed as mean. The percentage inhibition of bacterial growth was calculated using the formula.[18-21]

$$\%Inhibition = (1 - \frac{C}{T}) \times 100$$

Were,

C= Absorbance of Control

T=Absorbance of Test Sample

Table No. 11: Anti-TB Assay of derivatives PR4SII-A & PR4SII-B.

SR NO	SAMPLE CODE	Concentrations (µg/mL)	OD at 600 nm			Mean	% of Inhibition	IC_{50} (µg/mL)
1	Blank	-	0.061			-	-	-
2	Growth Control	-	1.455			-	-	-
3	Standard (Isoniazid)	20	0.889	0.891	0.893	0.891	38.76%	35.14
		40	0.672	0.675	0.678	0.675	53.61%	
		60	0.518	0.522	0.526	0.522	64.12%	
		80	0.389	0.394	0.39	0.391	73.13%	
		100	0.227	0.231	0.232	0.230	84.19%	
4	PR4SII-A	20	1.198	1.202	1.203	1.201	17.46%	73.74
		40	1.011	1.013	1.015	1.013	30.38%	
		60	0.81	0.812	0.814	0.812	44.19%	
		80	0.688	0.687	0.692	0.689	52.65%	
		100	0.553	0.556	0.559	0.556	61.79%	
5	PR4SII-B	20	1.144	1.146	1.148	1.146	21.24%	67.24
		40	0.921	0.924	0.927	0.924	36.49%	
		60	0.760	0.763	0.766	0.763	47.56%	
		80	0.662	0.665	0.668	0.665	54.30%	
		100	0.505	0.508	0.511	0.508	65.09%	

Graphical Data

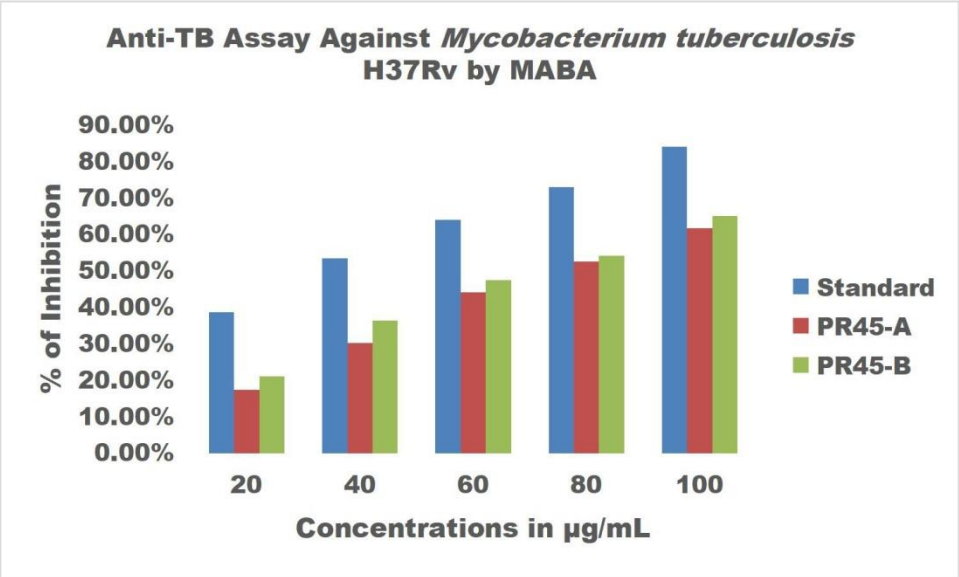

Figure No. 10: Anti-TB Against Mycobacterium tuberculosis H37Rv by MABA.

Images of the Activity

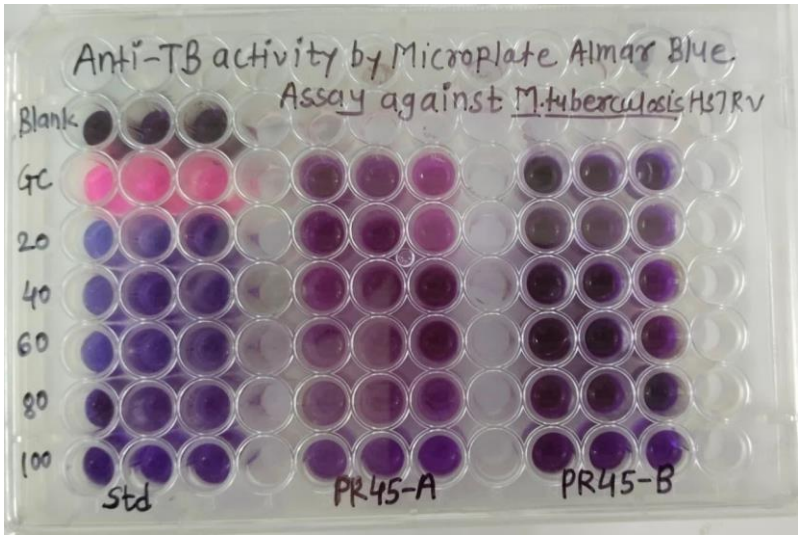

Figure No. 11: Anti-TB Activity by Microplate Almar Blue Assay Against Mycobacterium tuberculosis.

The antimycobacterial activity of the test samples PR4S-A, PR4S-B was evaluated against Mycobacterium tuberculosis H37Rv using the Microplate Alamar Blue Assay (MABA). Both test samples exhibited a concentration-dependent inhibition of mycobacterial growth over the tested concentration range (20-100µg/mL), as evidenced by the progressive reduction in absorbance values and corresponding increase in percentage inhibition. The reference drug Rifampicin demonstrated the highest antimycobacterial activity, producing 84.19% inhibition at 100 µg/mL with an IC_{50} value of 35.14 µg/mL**,** confirming the validity and sensitivity of the assay. Among the test samples, PR4SB exhibited greater antimycobacterial activity than PR4SA, achieving 65.09% inhibition at 100 µg/mL with an IC_{50} value of 67.24 µg/mL**,** whereas PR45-A showed 61.79% inhibition at 100 µg/mL with an IC_{50} value of 73.74 µg/mL**.** The lower IC_{50} value of PR45-B indicates that it possesses superior inhibitory potency compared with PR45-A Overall, the results indicate that both test sample possess moderate invitro anti mycobacterial activity against *M. tuberculosis* H37Rv. However, their efficacy was lower than that of Isoniazid.

CONCLUSION

In conclusion, both PR4SII-A and PR4SII-B demonstrate moderate anti-tuberculosis activity; however, PR4S-IIB emerged as the more promising candidate for further investigation and potential application in the treatment of tuberculosis.

ACKNOWLEDGMENT

We thank the Department of Pharmaceutical Chemistry, BLDEA's Shri Sanganabasava Mahaswamiji College of Pharmacy and Research Centre, Vijayapur, Karnataka, for providing all the required things used in this research.

Conflict of interest

All authors declare no conflict of interest.

REFERENCES

1. Bull JA, Mousseau JJ, Pelletier G, Charette AB. Synthesis of pyridine and dihydropyridine derivatives by regio-and stereoselective addition to N-activated pyridines. Chemical reviews, 2012 May 9; 112(5): 2642-713.
2. Marinescu M, Popa CV. Pyridine compounds with antimicrobial and antiviral activities. International journal of molecular sciences, 2022 May 18; 23(10): 5659.
3. Mohammad Abu-Taweel G, Ibrahim MM, Khan S, Al-Saidi HM, Alshamrani M, Alhumaydhi FA, Alharthi SS. Medicinal importance and chemosensing applications of pyridine derivatives: a review. Critical Reviews in Analytical Chemistry, 2024 Apr 2; 54(3): 599-616.
4. Sahu D, Sreekanth PR, Behera PK, Pradhan MK, Patnaik A, Salunkhe S, Cep R. Advances in synthesis, medicinal properties and biomedical applications of pyridine derivatives: A comprehensive review. European Journal of Medicinal Chemistry Reports, 2024 Dec 1; 12: 100210.
5. Singh P, Kumar A, Sharma P, Chugh S, Kumar A, Sharma N, Gupta S, Singh M, Kidwai S, Sankar J, Taneja N. Identification and optimization of pyridine carboxamide-based scaffold as a drug lead for Mycobacterium tuberculosis. Antimicrobial Agents and Chemotherapy, 2024 Feb7; 68(2): e00766-23.
6. Sabt A, Korycka-Machala M, Kassem AF, The Son N, Ha NX, Brzostek A, Thabit MG, Kawka M, Dziadek B, Elshamy AI, Atwa AM. Investigation of Potent Anti-Mycobacterium tuberculosis Agents Derived from Pyridine Derivatives Targeting the Enoyl Acyl Carrier Protein Reductase (InhA): Design, Synthesis, and Computational Analysis. Drug Design, Development and Therapy, 2026 Dec 31: 1-7.
7. Xia X, Shen J, Dai J, Arumuagam K, Rajalakshmi K, Dinakarkumar Y, Theivendren P, Muthusamy S, Zhu D, Yuan H. Design, synthesis, bioactivity evaluation, and molecular

modeling of pyridin-2-yl-pyrimidine: potential antimicrobial and anti-tuberculosis agents. Bioorganic Chemistry, 2025 Oct 28; 109167.

8. Mdluli K., Kaneko T. Tuberculosis drug discovery and emerging targets. Ann N Y Acad Sci, *20*11; 1213: 56–75.
9. Samanta S, Kumar S, Aratikatla EK, Ghorpade SR, Singh V. Recent developments of imidazo[1,2-a] pyridine analogues as antituberculosis agents. RSC Medicinal Chemistry, 2023; 14: 644-657. DOI: 10.1039/D3MD00019B
10. Kitchen D. B., Decornez H, Furr JR, Bajorath J. Docking and scoring in virtual screening for drug discovery: methods and applications. Nature Reviews Drug Discovery, *20*04; 3(11): 935–949.
11. World Health Organization. Global Tuberculosis Report 2024. Geneva: WHO, 2024.
12. Patel H, Nagani A, Patel M, Patel M, Yadav MR. Design, synthesis and biological evaluation of some imidazo [1, 2-a] pyridine derivatives as anti-tubercular agents: an in silico–in vitro approach. Journal of Biomolecular Structure and Dynamics, 2026 Jan 2; 44(1): 202-19.
13. .Shubrem AS, Mahdi SA, Hashim DA, Jwad RS, Abdullah MM, Abdulhaleem FA, Alyami MS, Jawad SF, Al-Mashhadani MH. Synthesis and Characterization of a Novel Series of Pyridine Derivatives and Their Antibacterial Activity. Iranian Journal of Science, 2026 Apr; 50(2): 511-24.
14. Abdin MM, Suleiman M, Amran SI, Al-Maqtari HM, Kawsar SM, Jamalis J. Therapeutic Potentials of Pyridine Derivatives, Highlighting the Synthetic Pathway, Biological Activity, and Structure-activity Relationship: A Mini-Review. Mini-Reviews in Medicinal Chemistry, 2026.
15. Tejaswani P, Das D, Kumar S, Kundu A, Jahan K, Jain R, Ahmed S. Advances in Five-Membered Heterocyclic Scaffolds as Anti-Tuberculosis Agents: A Decade of Discovery. Archiv der Pharmazie, 2026 Feb; 359(2): e70207.
16. Ganeshmurthy T, Ancy RP, Ganesmoorthy S, Gowri M. Evaluation of the Antitubercular Potential of Isoniazid: A Hydrazide Derivative. Russian Journal of Bioorganic Chemistry, 2026 Feb; 52(1): 6.
17. Krieger IV, Sukheja P, Yang B, Tang S, Selle D, Woods A, Engelhart C, Kumar P, Harbut MB, Liu D, Tsuda B. SuFEx-based antitubercular compound irreversibly inhibits Pks13. Nature, 2025 Sep 18;645(8081): 755-63.

18. Bükülmez G, Kasımoğulları R. Synthesis and reactions of pyridine and pyrimidine derivatives: developments of the last 10 years. Journal of the Iranian Chemical Society, 2026 Jan; 23(1): 2.
19. Chaskara PK, Somani RR. a review of structural features in novel molecules evaluated for antitubercular activity. Indian Drugs, 2025 May 1; 62(5).
20. Collins, L. A., & Franzblau, S. G. (1997). Microplate Alamar Blue assay versus BACTEC 460 system for high-throughput screening of compounds against Mycobacterium tuberculosis and Mycobacterium avium. Antimicrobial Agents and Chemotherapy, 41(5): 1004–1009. https://doi.org/10.1128/AAC.41.5.1004
21. Franzblau, S. G., Witzig, R. S., McLaughlin, J. C., Torres, P., Madico, G., Hernandez, A., Degnan, M. T., Cook, M. B., Quenzer, V. K., Ferguson, R. M., & Gilman, R. H. (1998). Rapid, low-technology MIC determination with clinical Mycobacterium tuberculosis isolates by using the Microplate Alamar Blue Assay. Journal of Clinical Microbiology, 36(2): 362–366. https://doi.org/10.1128/JCM.36.2.362-366.1998.